Available online at www.sciencedirect.com
ScienceDirect
Ceramics International 34 (2008) 773–777
CERAMICS INTERNATIONAL
www.elsevier.com/locate/ceramint

# Bismuth sodium titanate based lead-free ultrasonic transducer for microelectronics wirebonding applications

H.L.W. Chan [a,*], S.H. Choy [a], C.P. Chong [b], H.L. Li [b], P.C.K. Liu [b]

[a] Department of Applied Physics and Materials Research Centre, The Hong Kong Polytechnic University, Hunghom, Kowloon, Hong Kong, China
[b] ASM Assembly Automation Ltd., 12/F, Watson Centre, 16 Kung Yip Street, Kwai Chung, Hong Kong, China

Available online 2 October 2007

**Abstract**

Bismuth sodium titanate based lead-free piezoelectric ceramic $0.885(Bi_{1/2}Na_{1/2})TiO_3$–$0.05(Bi_{1/2}K_{1/2})TiO_3$–$0.015(Bi_{1/2}Li_{1/2})TiO_3$–$0.05BaTiO_3$ (BNKLBT-1.5) rings (OD = 12.7mm, ID = 5.1 mm and 2.3 mm thick) were fabricated and characterized. Four ceramic rings were sandwiched between front and back metal plates to form a pre-stressed piezoelectric sandwich transducer and used as the driving element of an ultrasonic wirebonding transducer and the performance of the transducer was evaluated. The BNKLBT-1.5 transducer, when fitted with titanium front and back plates, was found to have axial vibration comparable to that of PZT transducer thus showing that BNKLBT-1.5 has the potential to be used in fabricating lead-free ultrasonic wirebonding transducers.


*Keywords:* C. Piezoelectric properties; D. $BaTiO_3$ and titanates; Ultrasonic transducer

## 1. Introduction

Lead zirconate titanate [$Pb(Zr,Ti)O_3$, abbreviated as PZT] ceramics are dominant piezoelectric materials due to their superior piezoelectric properties. However, the high PbO vaporization and contamination during processing and disposal cause a crucial environmental pollution. For this reason, it is desirable to use lead-free piezoelectric ceramics to replace PZT and increased attentions have been drawn to the investigation of lead-free piezoelectric ceramics and devices [1].

$(Bi_{1/2}Na_{1/2})TiO_3$ (abbreviated as BNT) is an important lead-free ceramic with perovskite structure discovered by Smolenskii et al. in 1960 [2]. BNT has a relatively large remanent polarization of $P_r = 38\ \mu C/cm^2$ and a high coercive field of $E_c = 7.3$ MV/m at room temperature. It also has a high Curie temperature ($T_c = 320\ ^\circ C$) [3,4]. In addition, BNT reveals an anomaly in dielectric properties at about 200 °C referred to as depolarization temperature $T_d$. The drawback of BNT is its high leakage current during poling which gives rise to ineffective poling. Various attempts have been made to obtain useful BNT-based lead-free piezoelectric ceramics by incorporating $BaTiO_3$, $(Bi_{0.5}K_{0.5})TiO_3$, $NaNbO_3$, $BiFeO_3$ and $Ba(Cu_{0.5}W_{0.5})O_3$ [5–8] to form binary systems which are easier to pole or having enhanced piezoelectric properties. A ternary system which combined both $(Bi_{1/2}Na_{1/2})TiO_3 - (Bi_{1/2}K_{1/2})TiO_3 - BaTiO_3$ (BNKBT) was first reported by H. Nagata et al. [9] and further investigated by our group [10,11] and other researchers [12,13]. These systems have relatively high piezoelectric and good dielectric properties for compositions near the MPB. We found that BNKBT-5 has the optimum composition within our study and we have applied this material in different applications and found that the performance is comparable to PZT [14,15]. Based on BNKBT-5, further modification was made by doping bismuth lithium titanate [$(Bi_{1/2}Li_{1/2})TiO_3$, BLT]. Both the electromechanical coupling factors and mechanical quality factors are greatly improved and the dielectric loss has been reduced after doping a suitable amount of BLT.

Piezoelectric ultrasonic transducer is an important application for piezoelectric materials as it converts electrical energy to mechanical energy or vice versa. In this work, BLT modified BNKBT ceramic, namely BNKLBT-1.5, with the composition of $(0.90\text{-}x)(Bi_{1/2}Na_{1/2})TiO_3$–$0.05(Bi_{1/2}K_{1/2})TiO_3$–$x(Bi_{1/2}Li_{1/2})TiO_3$–$0.05BaTiO_3$ ($x = 0.015$) was prepared. An ultrasonic transducer used for bonding aluminum wires onto integrated circuit (IC) chips was fabricated using four BNKBLT ceramic

* Corresponding author. Tel.: +852 2766 5692; fax: +852 2766 1202.
*E-mail address:* apahlcha@inet.polyu.edu.hk (H.L.W. Chan).

0272-8842/$34.00 
doi:10.1016/j.ceramint.2007.09.085

rings. A commercial FEM code ANSYS was used to analyze the vibration characteristics of the transducer and compared to experimental results. The performance of the prototype BNKLBT-1.5 transducer was compared with a transducer composed of PZT APC840 rings (supplied by American Piezo Ceramics Ltd.).

## 2. Sample preparation

The conventional mixed oxide technique was used to prepare BNKLBT-1.5 ceramics. Reagent grade $Bi_2O_3$, $Na_2CO_3$, $BaCO_3$, $K_2CO_3$, $Li_2CO_3$ and $TiO_2$ were used as raw materials. They were weighed according to the formula $0.885(Bi_{1/2}Na_{1/2})TiO_3$–$0.05(Bi_{1/2}K_{1/2})TiO_3$–$0.015(Bi_{1/2}Li_{1/2})TiO_3$–$0.05BaTiO_3$. The powder was ball-milled in ethanol using zirconia balls for 10 h. Calcination was conducted at 800 °C for 2 h. After calcinations, the mixture was dried and added with PVA as a binder for granulation. The granulated powders were pressed into rings. The compacted rings were sintered at 1170 °C for 2 h in air. Silver paste was applied on both surfaces of the rings and fired at 650 °C as electrodes. The samples were poled in silicone oil at room temperature under 4.0 MV/m for 10 min.

## 3. Material properties of BNKLBT-1.5 lead-free ceramics and PZT APC840 ceramics

Density of the sintered samples was measured using the Archimedes principle. The $d_{33}$ coefficient of the poled samples was measured at 100 Hz using a $d_{33}$ m (ZJ-30 PIEZO $d_{33}$ m). The resonance measurements were conducted using an HP 4294A impedance analyzer. The electromechanical coupling factors were calculated from the resonance and anti-resonance frequency following the IEEE standards. Dielectric properties of the samples were determined using the HP 4294A impedance analyzer at 1 kHz. Table 1 summarizes the measured materials properties.

Table 1
Materials properties of BNKLBT-1.5 and APC 840 ceramics

| Sample | APC840 | BNKLBT-1.5 |
|---|---|---|
| Density (kg $m^{-3}$) | 7516 | 5780 |
| Relative permittivity $\varepsilon_r$ | 1112 | 766 |
| Tan $\delta$ loss (%) | 0.75 | 1.61 |
| $k_t$ | 0.357 | 0.524 |
| $k_p$ | 0.59 | 0.328 |
| $k_{31}$ | 0.32 | 0.188 |
| $s_{11}^E$ ($\times 10^{-12}$ $m^2$ $N^{-1}$) | 10.62 | 8.369 |
| $s_{12}^E$ ($\times 10^{-12}$ $m^2$ $N^{-1}$) | −3.144 | −2.33 |
| $s_{11}^D$ ($\times 10^{-12}$ $m^2$ $N^{-1}$) | 9.552 | 8.073 |
| $s_{12}^D$ ($\times 10^{-12}$ $m^2$ $N^{-1}$) | −4.209 | −2.626 |
| $Q_{M(radial)}$ | 774.5 | 142.1 |
| $d_{33}$ (pC/N) | 254 | 163 |
| $Y_{11}^E$($\times 10^9$ $Nm^{-2}$) | 94.22 | 110.49 |
| Poisson's ratio | 0.395 | 0.278 |
| Acoustic Impedance $Z_a$ (MRayl) In thickness (poling) direction | 35.7 | 26.41 |

## 4. Prototype ultrasonic wirebonding transducer

The transducer is operated at ~63 kHz and equipped with a wedge tool for wedge bonding. The transducer can basically be divided into three sections, including a driver, a horn and a wedge as shown in Fig. 1. The driver is used to generate the ultrasonic vibration during the bonding and it is a Langevin sandwich-type transducer. The driver is formed by four piezoelectric rings, connected electrically in parallel and mechanically in series with thin ring electrodes inserted in between, and are sandwiched between front and back metal plates by a central pre-stressed bolt. The front plate of the driver has a screw on one side which can screw-connect with the horn. The horn has an exponential profile which couples and amplifies the axial vibration of the driver to provide a maximum vibration across the horn tip. The front and back plates of the PZT APC 840 transducer (Transducer A) are made of stainless steel (S.S.) and those of the BNKLBT-1.5 transducer (Transducer B) are made of titanium alloy (Ti).

## 5. Finite element model for the prototype transducer

As the transducer has axial-symmetry about its central ($z$) axis, the characteristics of the transducer is modelled as 360° elements with symmetry boundary condition applied about the $z$ axis. The schematic diagram of the 360° finite element model for Transducer B is shown in Fig. 2. The advantage of using a full model is that all possible resonance modes including both the flexural and axial modes can be found. The material properties of APC840, BNKLBT-1.5 and the metal components were used in the simulation. The loss factors were not included in the model. Linear and anisotropic properties are assumed for the piezoelectric elements while linear and isotropic properties are used for the metal components. For ease of meshing, the thread of the pre-stressed screw has been ignored. Simplification has been made to the front plate and screw where the thread and threaded bore have been simplified. The ring-shaped copper electrodes are assumed to be very thin, and they have not

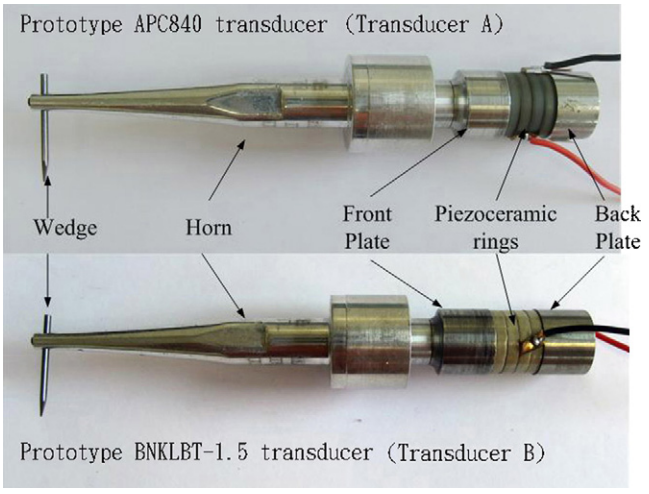


Fig. 1. Photograph of the prototype ultrasonic transducers with different driving elements, PZT APC 840 (Transducer A) and BNKLBT-1.5 (Transducer B).

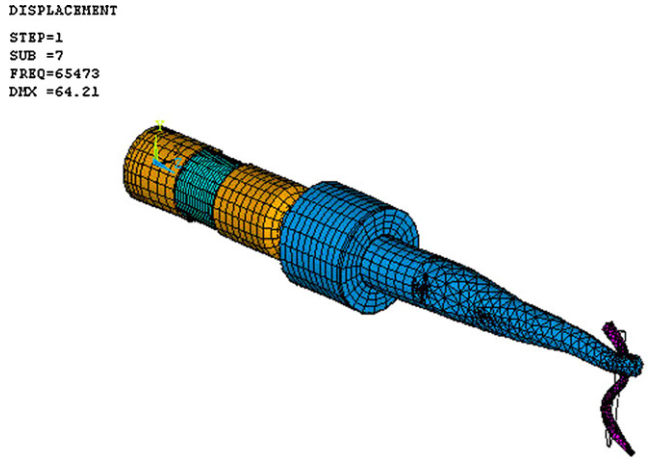


Fig. 2. Finite element model of a 65 kHz ultrasonic transducer (Transducer B) shown in Fig. 1. The full model includes the screw, barrel, and wedge.

been taken into account. All components in the assembly are assumed to have perfect mechanical coupling to each other. Good convergence of the results has been reached by successively increasing the number of solid elements and nodes in order to approximate the exact numerical solution to within 5% for frequencies up to 150 kHz. The lowest 100 natural frequencies and mode shapes of lead-free transducer have been computed using a commercial finite element software package ANSYS® version 9.0.

The calculated axial operating frequency in Transducer A and Transducer B are 63.89 and 65.47 kHz, respectively, which are in good agreement with the measured value of 60.58 kHz (Transducer A) and 65.26 kHz (Transducer B) (Fig. 3). Physically, a pure axial excitation produces an axial front-to-back motion in the ultrasonic horn, which in turn, causes a large displacement at the tip of the wedge. As this motion is essentially in line with the wire to be bonded, hence the axial mode is the most desirable resonance mode.

## 6. Prototype ultrasonic transducer

The frequency impedance/phase spectra of the prototype transducers are shown in Fig. 3. Transducer A has the strongest resonance at ∼60 kHz and Transducer B has the strongest resonance at ∼65 kHz, identified as the second axial mode, is the designated working mode of the prototype transducer with the length of the horn and the cylindrical coupler equals to one longitudinal wavelength λ (the whole transducer including the driver is equal to 1.5λ). For frequencies ranging from 40 Hz to 800 kHz, the prototype transducers (Fig. 3) have little prominent resonance although some weak higher order modes can still be found in this frequency range. Some of the measured parameters of the prototype transducers are listed in Table 2. The difference in the frequency of the calculated and measured thickness mode vibration $f_T$ may be due to the inaccuracy in the material parameters.

The vibration characteristics of the ultrasonic transducer were measured using a Polytec laser Doppler vibrometer connected to a digital oscilloscope (HP54522A). The transducer was affixed with similar clamping condition to the holder, and a constant input power of 0.1 W was used to drive the transducer. The waveform of the axial displacement at the front of the wedge tip was measured under the same input power. Table 2 summarizes the vibration amplitude measurements at different locations on the transducers. During the bonding action, envelop of sine waves corresponding to the transducer resonance frequency was received by the transducer. The

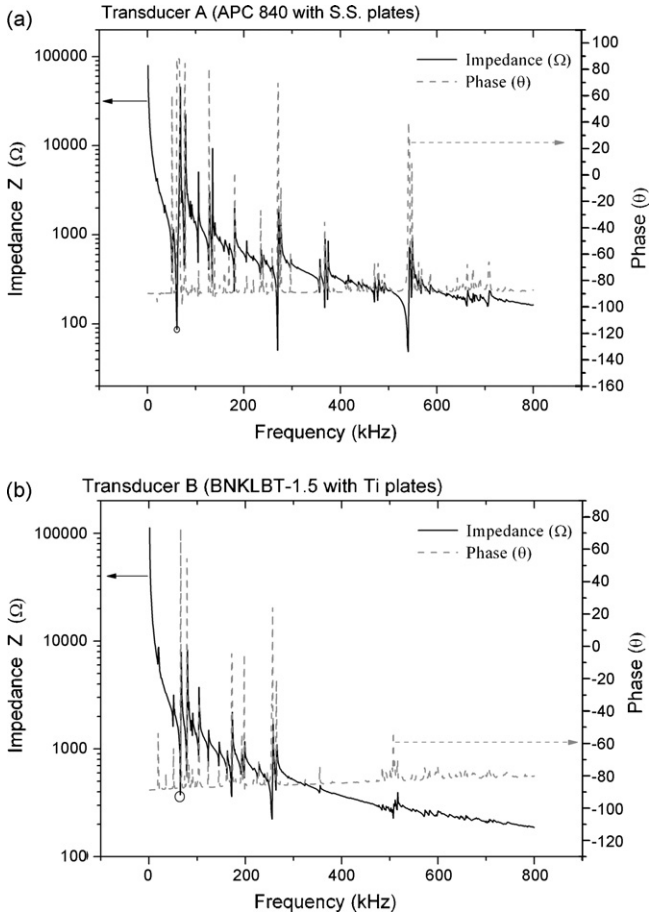


Fig. 3. Plots of electrical impedance (solid line) and phase angle (dotted line) vs. frequency for (a) Transducer A and (b) Transducer B.

Table 2
Characteristics of Transducer A (PZT) and Transducer B (BNKLBT-1.5)

| | Transducer A | Transducer B |
|---|---|---|
| Resonance frequency, $f_r$ (kHz) | 60.58 | 65.02 |
| Impedance, $Z_m$ (Ω) | 16.84 | 135.00 |
| Mechanical quality factor, $Q_m$ | 405.64 | 295.99 |
| Electromechanical coupling factor, $k_{eff}$ | 0.513 | 0.228 |
| Average vibration amplitude at wedge tip front (μm) | 1.693 | 1.669 |
| Average vibration amplitude at wedge tip side (μm) | 0.191 | 0.082 |
| F/S ratio | 8.86 | 20.23 |
| Averaged rising time, $t_r$ (ms) | 5.45 | 7.48 |
| Averaged falling time, $t_f$ (ms) | 7.76 | 5.91 |

transducer needs a responding time to increase/decrease the vibration amplitude to the desired level. That corresponding times are called the voltage rise time and fall time. Transducer B has a longer voltage rise time and shorter fall time than that of the PZT transducer (Table 2). Transducer A has very high axial vibration amplitude which exceeds 1.5 μm. But it has relatively large lateral displacement and thus the ratio of axial displacement to lateral displacement is relatively small, especially the F:S ratio. The locus of vibration measured on the wedge tip will become an ellipse. When the lateral displacement is large, the bond width will increase and that is not desirable. Hence, to maintain a high F:S ratio is important for miniaturization as a narrow bond width can be achieved. The lateral vibration can effectively be reduced by using driving materials with lower electromechanical coupling coefficient in the lateral direction ($k_{31}$). Fabricating 1–3 ceramic/polymer composites is a good way to reduce $k_{31}$ to enhance the performance of the transducer [16]. Here, using BNKLBT-1.5, which has a much smaller $k_{31}$ than the PZT APC 840, can also reduce the energy transfer to the lateral vibration and thus improve the ratio between axial vibration to lateral vibration. Transducer B has large axial vibration and relatively small lateral vibration. The large axial vibration is mainly due to the design of the driver which is related to the acoustics impedance between the materials. Ultrasonic wirebonding transducer is a device operating at 1.5λ axial vibrational mode, which is mainly contributed by the axial vibration of the driver. The axial vibration of the driver is generated by the thickness mode vibration of the driving elements (piezoelectric ceramics). By converse piezoelectric effect, piezoelectric ceramics convert electrical energy to mechanical energy. The mechanical energy is the source of the vibration, firstly transferred to the metal plates in the driver and then transferred to the horn. The acoustic impedance between the piezoelectric ceramics and the metal plates (front and back plates) is a critical factor that determined the efficiency of energy transfer in the ultrasonic wirebonding transducer. An increase in the mismatch of acoustics impedance results in a decrease in efficiency. The

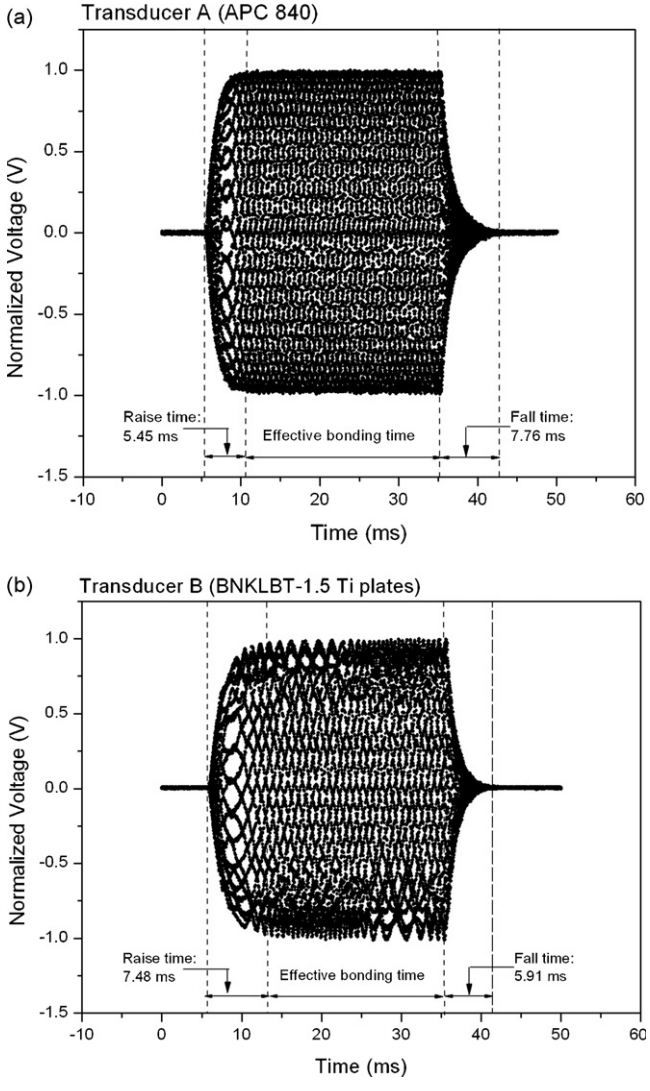


Fig. 4. Axial vibration response of (a) Transducer A and (b) Transducer B as measured at the wedge tip.

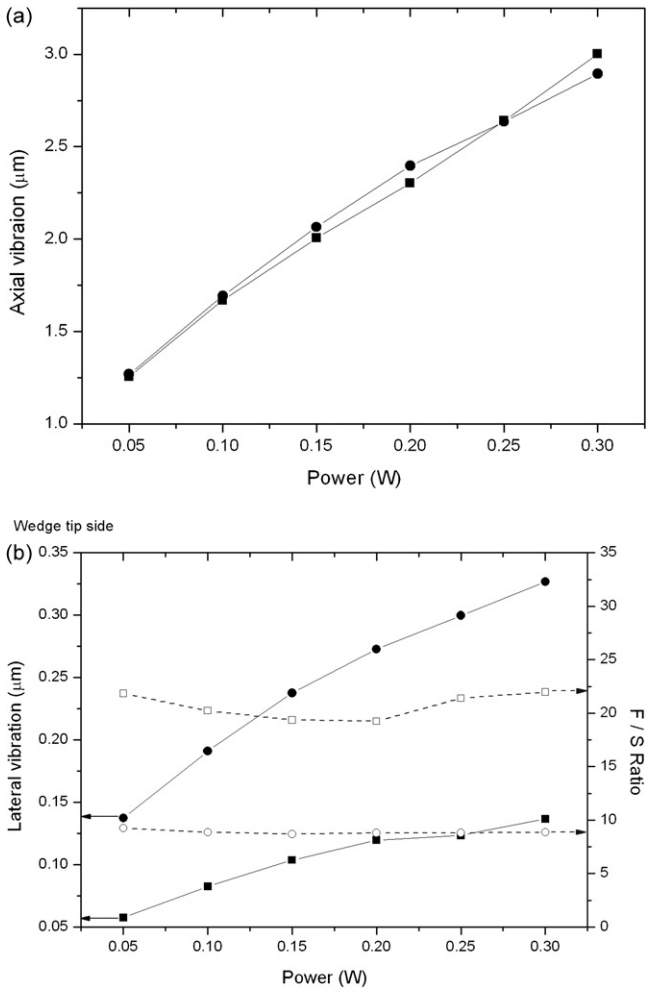


Fig. 5. Plots of (a) the axial vibration of the horn tip and the axial vibration of the wedge tip, (b) lateral vibration of the wedge tip and F/S ratio vs. the input power for Transducer A (circle) and Transducer B (square).

acoustic impedance of the driving materials in the thickness mode is listed in Table 1. The acoustic impedance of stainless steel and titanium alloy is 45.7 and 27.3 MRayl, respectively [17]. The acoustic impedance of titanium alloy is close to that of BNKLBT-1.5, hence vibration energy can be transferred more effectively which greatly improves the axial vibration performance of Transducer B Fig. 4.

The output power of the ultrasonic wirebonding transducer can be varied in different bonding condition and the output power is determined by the electrical input power. It is important to have a transducer with high stability for industrial applications. The vibrational performance of different prototype transducers with varied input power from 0.05 to 0.3 W is shown in Fig. 5. The axial vibration of the horn tip and wedge tip is approximately linearly proportional to the input power, but the lateral vibration of the wedge tip is different in different prototype transducers. It is observed that lead-based transducer has higher axial vibration and high lateral vibration and thus has a relatively low F:S ratio which is because PZT has a high $k_{31}$. Transducer B has a steady F:S ratios over the measuring range and has a better performance in reducing the lateral vibration than the lead-based transducer.

## 7. Conclusions

The lead-free material BNKLBT-1.5 has been fabricated successfully and its material parameters were characterized. The ceramic rings were used as the driving element in the ultrasonic transducer. In the vibration characterization, the BNKLBT-1.5 transducer was found to have an axial vibration comparable to that of PZT transducer. In addition, the lateral vibration of the lead-free transducer is 1/2 that of the PZT transducer. This indicates that the lead-free ceramics, BNKLBT-1.5, can be a potential candidate for use to fabricate ultrasonic wirebonding transducers.

## Acknowledgements

The authors would like to acknowledge supports from the Hong Kong Research Grants Council (PolyU 5317/04E), the Innovation and Technology Fund (ITF GHS/066/04) of the HKSAR government and the Center for Smart Materials of The Hong Kong Polytechnic University.

## References

[1] T. Takenaka, Movement of study on lead-free piezoelectric materials, Ultrason. Technol. 8 (2001) 2.
[2] G.A. Smolenskii, V.A. Isupov, A.I. Agranovskaya, N.N. Krainik, New ferroelectrics of complex composition, Sov. Phys.-Soild State (Engl. Transl.) 2 (11) (1961) 2651.
[3] J. Suchanicz, K. Roleder, A. Kania, J. Handerek, Electrostrictive strain and pyroeffect in the region of phase coexistance in $Na_{0.5}Bi_{0.5}TiO_3$, Ferroelectrics 77 (1988) 107.
[4] M.S. Hagiyev, I.H. Ismaizade, A.K. Abiyev, Pyroelectric properties of $(Bi_{1/2}Na_{1/2})TiO_3$ ceramics, Ferroelectrics 56 (1984) 215.
[5] T. Takenaka, K.I. Maruyama, K. Sakata, $(Bi_{0.5}Na_{0.5})TiO_3$-$BaTiO_3$ system for lead-free piezoelectric ceramics, Jpn. J. Appl. Phys. Part 1-Reg. Pap. Short Notes Rev. Pap. 30 (9B) (1991) 2236.
[6] A. Sasaki, T. Chiba, Y. Mamiya, E. Otsuki, Dielectric and piezoelectric properties of $(Bi_{0.5}Na_{0.5})TiO_3$-$(Bi_{0.5}K_{0.5})TiO_3$ systems, Jpn. J. Appl. Phys. Part 1-Reg. Pap. Short Notes Rev. Pap. 38 (9B) (1999) 5564.
[7] H. Nagata, N. Koizumi, T. Takenaka, Lead-free piezoelectric ceramics of $(Bi_{1/2}Na_{1/2})TiO_3$–$BiFeO_3$ System, Key Eng. Mater. 169–170 (1999) 37.
[8] X.X. Wang, H.L.W. Chan, C.L. Choy, $(Bi_{0.5}Na_{0.5})TiO_3$-$Ba(Cu_{0.5}W_{0.5})O_3$ lead-free piezoelectric ceramics, J. Am. Ceram. Soc. 86 (10) (2003) 1809.
[9] H. Nagata, M. Yoshida, Y. Makiuchi, T. Takenaka, Large piezoelectric constant and high Curie temperature of lead-free piezoelectric ceramic ternary system based on bismuth sodium titanate-bismuth potassium titanate-barium titanate near the morphotropic phase boundary, Jpn. J. Appl. Phys. Part 1-Reg. Pap. Short Notes Rev. Pap. 42 (12) (2003) 7401.
[10] X.X. Wang, X.G. Tang, H.L.W. Chan, Electromechanical and ferroelectric properties of $(Bi_{1/2}Na_{1/2})TiO_3$-$(Bi_{1/2}K_{1/2})TiO_3$-$BaTiO_3$ lead-free piezoelectric ceramics, Appl. Phys. Lett. 85 (1) (2004) 91.
[11] X.X. Wang, S.H. Choy, X.G. Tang, H.L.W. Chan, Dielectric behavior and microstructure of $(Bi_{1/2}Na_{1/2})TiO_3$ – $(Bi_{1/2}K_{1/2})TiO_3$ – $BaTiO_3$ lead-free piezoelectric ceramics, J. Appl. Phys. 97 (2005) 104101.
[12] Y. Makiuchi, R. Aoyagi, Y. Hiruma, H. Nagata, T. Takenaka, $(Bi_{1/2}Na_{1/2})TiO_3$-$(Bi_{1/2}K_{1/2})TiO_3$-$BaTiO_3$-based lead-free piezoelectric ceramics, Jpn. J. Appl. Phys. Part 1-Reg. Pap. Short Notes Rev. Pap. 44 (6B) (2005) 4350.
[13] Y. Hiruma, H. Nagata, T. Takenaka, Phase transition temperatures and piezoelectric properties of $(Bi_{1/2}Na_{1/2})TiO_3$-$(Bi_{1/2}K_{1/2})TiO_3$-$BaTiO_3$ lead-free piezoelectric ceramics, Jpn. J. Appl. Phys. Part 1-Reg. Pap. Short Notes Rev. Pap. 45 (9B) (2006) 7409.
[14] S.H. Choy, X.X. Wang, C.P. Chong, H.L.W. Chan, P.C.K. Liu, C.L. Choy, $0.90(Bi_{1/2}Na_{1/2})TiO_3$-$0.05(Bi_{1/2}K_{1/2})TiO_3$-$0.05BaTiO_3$ transducer for ultrasonic wirebonding applications, Appl. Phys. A-Mater. Sci. Proc. 84 (2006) 313.
[15] S.H. Choy, X.X. Wang, H.L.W. Chan, C.L. Choy, Study of compressive type accelerometer based on lead-free BNKBT piezoceramics, Appl. Phys. A-Mater. Sci. Proc. 82 (2006) 715.
[16] C.P. Chong, H.L. Li, H.L.W. Chan, P.C.K. Liu, Study of 1–3 composite transducer for ultrasonic wirebonding application, Ceram. Int. 30 (2004) 1141.
[17] Onda Corporation, http://www.ondacorp.com/tecref_acoustictable.html.